Journal of Hazardous Materials 184 (2010) 392–399

Contents lists available at ScienceDirect

Journal of Hazardous Materials

journal homepage: www.elsevier.com/locate/jhazmat

Effective removal of Cu (II) ions from aqueous solution by amino-functionalized magnetic nanoparticles

Hao Yong-Mei[a,*], Chen Man[a], Hu Zhong-Bo[b,*]

[a] College of Chemistry and Chemical Engineering, Graduate University of Chinese Academy of Sciences, 19(A) Yu Quan Road, Beijing 100049, China
[b] College of Materials and Photoelectric Technology, Graduate University of Chinese Academy of Sciences, 19(A) Yu Quan Road, Beijing 100049, China

ARTICLE INFO

Article history:
Received 4 February 2010
Received in revised form 30 June 2010
Accepted 15 August 2010
Available online 21 August 2010

Keywords:
Copper
Removal
Amino-functionalized
Adsorption
Magnetic nanoparticle

ABSTRACT

A novel magnetic nano-adsorbent (MNP-NH_2) has been developed by the covalent binding of 1,6-hexadiamine on the surface of Fe_3O_4 nanoparticles for removal of Cu^{2+} ions from aqueous solution. Various factors affecting the uptake behavior such as contact time, temperature, pH, salinity, amount of MNP-NH_2 and initial concentration of Cu^{2+} were investigated. The kinetics was evaluated utilizing the Lagergren pseudo-first-order, pseudo-second-order, Elovich and intra-particle diffusion models. The equilibrium data were analyzed using Langmuir, Freundlich, and Dubinin–Radushkevich isotherms. The adsorption was relatively fast and the equilibrium was established within 5 min, and its kinetics followed the pseudo-second-order mechanism, evidencing chemical sorption as the rate-limiting step of sorption mechanism. The best interpretation for the equilibrium data was given by Langmuir isotherm, and the maximum adsorption capacities was 25.77 mg g^{-1} at pH 6, and 298 K. Thermodynamic parameters showed that the adsorption process was spontaneous, endothermic and chemical in nature. The successive adsorption–desorption studies indicated that the MNP-NH_2 sorbent kept its adsorption and desorption efficiencies constant over 15 cycles. Importantly, MNP-NH_2 was able to remove 98% of Cu^{2+} from polluted river and tap water.

1. Introduction

Copper is widely used in many industries, such as electroplating, paint, metal finishing, electrical, fertilizer, wood manufacturing and pigment industries. Rapid development of these industries has led to accumulation of Cu^{2+} ions in the environment. Unlike some organic pollutants, copper and some other toxic heavy metals are non-biodegradable and can exist for a long time in natural environment. If the level of Cu^{2+} ions is beyond the tolerance limit, it will cause serious environmental and public health problems. It is necessary to remove Cu^{2+} ions from industrial effluents prior to their discharge. Up to now, numerous technologies have been developed, including chemical precipitation [1], ion exchange [2], liquid–liquid extraction [3], electrodialysis [4], biosorption [5–7] and so on. Each method has its inherent limitations. For example, it is well known that chemical precipitation generates large amounts of sludge and secondary wastewater requiring treatment.

In recent years, for the treatment of Cu (II)-rich effluents, considerable attention has been concentrated on the removal of Cu^{2+} ions by adsorption method because it is simple, relative low-cost, effective and flexible in design and operation. Up to now, numerous adsorbents have been developed including activated carbon [8], carbon nanotubes [9], chitosan [10], lignocelluloses [11], synthetic porous inorganic materials [12], natural inorganic minerals [13,14], zero-valent iron [15], functionalized polymers [16,17] and so on. However, most of these adsorbents show unsatisfied adsorption capacity due to diffusion limitation or the lack of enough active surface sites, and some problems, including high cost, difficulties of separation and regeneration of adsorbents from wastewater, and secondary wastes, have to be faced. So, it is very important to develop novel adsorbents with large adsorptive surface area, low diffusion resistance, high adsorption capacity and fast separation for large volumes of solution. Considering these characteristics, nanomaterials attracted much attention and various nano-adsorbents have been exploited to remove heavy metal ions from solution. Nano-alumina [18], nanomagnets coated by EDTA [19], carbon nanotube [20] and hydroxyapatite nanoparticle [21] have been used as adsorbent for Cu^{2+} removal, and the experimental results indicate that these materials have high adsorption efficiency.

Usually it is difficult to separate adsorbents fast from large volumes of solution, while magnetic adsorbents can circumvent this problem because they can be separated easily from solution by an external magnetic field. Therefore, adsorbents combining nanotechnology and magnetic separation technique would remove heavy metal ions in perfect performance. Up to now, sev-

* Corresponding author. Tel.: +86 10 88256414; fax: +86 10 88256093.
E-mail addresses: ymhao@gucas.ac.cn (Y.-M. Hao), huzq@gucas.ac.cn (Z.-B. Hu).

0304-3894/$ – see front matter © 2010 Elsevier B.V. All rights reserved.
doi:10.1016/j.jhazmat.2010.08.048

eral magnetic nanomaterials, including maghemite nanoparticles [22,23], Fe_3O_4 magnetic nanoparticles [24,25], Fe_3O_4 nanoparticles functionalized with some compounds, such as humic acid [26], amino-functionalized polyacrylic acid (PAA) [27], dimercaptosuccinic acid [28], gum arabic [29], polyvinyl acetate–iminodiacetic acid [30], and natural or modified chitosan [31,32], have been explored for the removal of copper ions. These magnetic nanoadsorbents were found to be cost-effective, simple to use, and environmental-sound compared to the present other adsorbents. However, these modified Fe_3O_4 nanoparticles were prepared in two or three steps, namely, magnetic core was prepared firstly and then coated with different organic shells [26–32].

It has been reported previously that amine-functionalized Fe_3O_4 nanoparticles could be prepared by a facile one-pot method using $FeCl_3{\cdot}6H_2O$ as single iron source [33], and the prepared nanoparticles were applied to immunoassays and magnetic resonance imaging in live mice. In this study, our aim is to prepare these amine-functionalized Fe_3O_4 nanoparticles (MNP-NH_2) and check their adsorption capability in removing Cu^{2+} from aqueous solution. The adsorption process has been investigated in detail, and both kinetic and thermodynamic features have been analyzed. Moreover, reusability of the prepared adsorbent was examined.

2. Experimental

Preparation and characterization of MNP-NH_2 were described in the Supporting Information.

2.1. Adsorption and desorption studies

The adsorption of Cu^{2+} ions by the amino-functionalized magnetite nanoparticles was investigated in aqueous solution at 25 °C. In general, the amino-functionalized magnetite nanoparticles (5.0 mg) were put into 50.0 mL of aqueous solution containing Cu^{2+} ions (10.0 mg L^{-1}), the mixture was adjusted to certain pH with NaOH or HCl and mixed by ultrasonication several minutes until the equilibrium was established. For removal of Cu^{2+} from real water, 5.0 mg of the as-prepared MNP-NH_2 was added into 50.0 mL of water. Then the MNP-NH_2 with adsorbed Cu^{2+} was separated from the mixture with a permanent hand-held magnet. The concentration of Cu^{2+} in the supernatant was measured by flame atomic absorption spectrometer (Ruili WFX-130). For comparison, the adsorption of Cu^{2+} by the naked Fe_3O_4 nanoparticles (MNP) was also investigated. To obtain the corresponding adsorption isotherms and thermodynamic parameters, solutions containing different initial concentration of Cu^{2+} (0.1, 1, 2, 3, 4, 5 mg L^{-1}) were treated with the same procedure as above-mentioned at different temperatures.

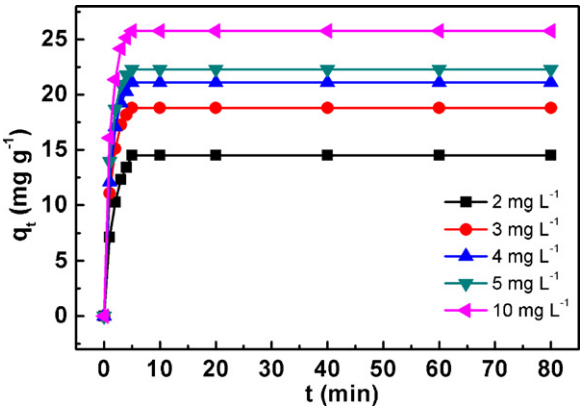

Fig. 1. Effect of contact time and initial metal concentration on sorption capacity of Cu^{2+} on MNP-NH_2 nanoparticles (pH 6.0, MNP-NH_2 dosage 0.1 g L^{-1}, temperature 25 °C).

Desorption of Cu^{2+} was performed by mixing 5 mg of copper ions-loaded MNP-NH_2 into 10 mL of HCl solution (0.1 mol L^{-1}), and sonicating for 1 min. Then, the MNP-NH_2 was separated from the solution by a permanent magnet and washed with distilled water three times, and dried for reuse. The consecutive adsorption–desorption process was carried out 15 times.

2.2. Statistical analysis

All the experiments were carried out in triplicate and data presented are the mean values from these independent experiments. Standard deviation and error bars are indicated wherever necessary.

3. Results and discussion

3.1. Adsorption kinetics

The adsorption kinetics information has a significant practical value. Rapid reaction time will facilitate smaller reactor volumes ensuring efficiency and economy. To examine the influence of time on Cu^{2+} adsorption, kinetics experiments were carried out by adding 5.0 mg of new prepared MNP-NH_2 to 50.0 mL solution containing 2.0, 3.0, 4.0, 5.0 or 10.0 mg L^{-1} Cu^{2+} at pH 6.0, 25 °C. The result shown in Fig. 1 indicated that adsorption equilibriums were reached within 5 min. This rapid adsorption indicated that the adsorption occurred mainly on the surface of the adsorbent, being similar with some previous results [26,31].

Moreover, Lagergren pseudo-first order [34], pseudo-second order [35], Elovich [36] and intra-particle diffusion [37] kinetic models have been used to examine experimental data. All kinetic equations are presented in Table 1, where q_e and q_t are the sorption capacity (mg g^{-1}) at equilibrium and at time t (min), k is the rate constant, and h is the initial sorption rate in pseudo-second-order model. In all regression cases, the sum of error squared (SSE) between the predicted values and the experimental data can be calculated by the following equation:

$$\mathrm{SSE} = \frac{\sqrt{\sum_{i=1}^{N}(q_{\mathrm{exp}} - q_{\mathrm{calc}})^2}}{N} \quad (1)$$

where the subscripts exp and calc are the experimental and calculated values of q, respectively. N is the number of measurements.

The Lagergren-first-order rate constants k_1 were calculated from the slope of Fig. 2(a). It was observed that k_1 increased with increasing initial Cu^{2+} concentration. The correlation coefficients were in the range of 0.9984–0.9997 (Table 2).

The pseudo-second order kinetic constant k_2 and q_e can be calculated from the intercept and slope of the plots of t/q_t *vs.* t (Fig. 2(b)). The rate constants k_2, the calculated equilibrium sorption capacities q_e(calc.), the initial sorption rate h, and the linear correlation coefficient values R^2 obtained by linear regression are listed in Table 2. For any c_0 value within the scope of investigation, the rate constant k_2 and initial sorption rate h increased with the increase of initial concentrations. This trend suggests that a chemisorptions reaction occurs between Cu^{2+} and NH_2 groups on the surface of MNP-NH_2.

The Elovich equation is often used to interpret the kinetics of sorption and successfully describe the predominantly chemical sorption on highly heterogeneous sorbents. In its linear Eq. (4), α is the initial adsorption rate (mg g^{-1} min^{-2}) and β is the desorption constant (g mg^{-1} min^{-1}). Here the relationships between q_t

Table 1
Mathematical equations in Cu^{2+} adsorption kinetics.

Kinetic models	Linear equations	Plot	Calculated coefficients
Lagergren pseudo-first-order	$\ln(q_e - q_t) = \ln q_e - k_1 t$ (2)	$\ln(q_e - q_t)$ *vs.* t	k_1 = −slope, $q_e = e^{\text{intercept}}$
Pseudo-second-order	$\frac{t}{q_t} = \frac{1}{k_2 q_e^2} + \frac{t}{q_e}$, $h = k_2 q_e^2$ (3)	t/q_t *vs.* t	k_2 = slope^2/intercept, q_e = 1/slope
Elovich	$q_t = \frac{1}{\beta}\ln(\alpha\beta) + \frac{1}{\beta}\ln(t)$ (4)	q_t *vs.* $\ln(t)$	$\alpha = e^{(\text{intercept/slope} - \ln(\beta))}$, β = 1/slope
Intra-particle diffusion	$q_t = k_{\text{intra}}(t)^{1/2} + C$ (5)	q_t *vs.* $t^{1/2}$	k_{intra} = slope

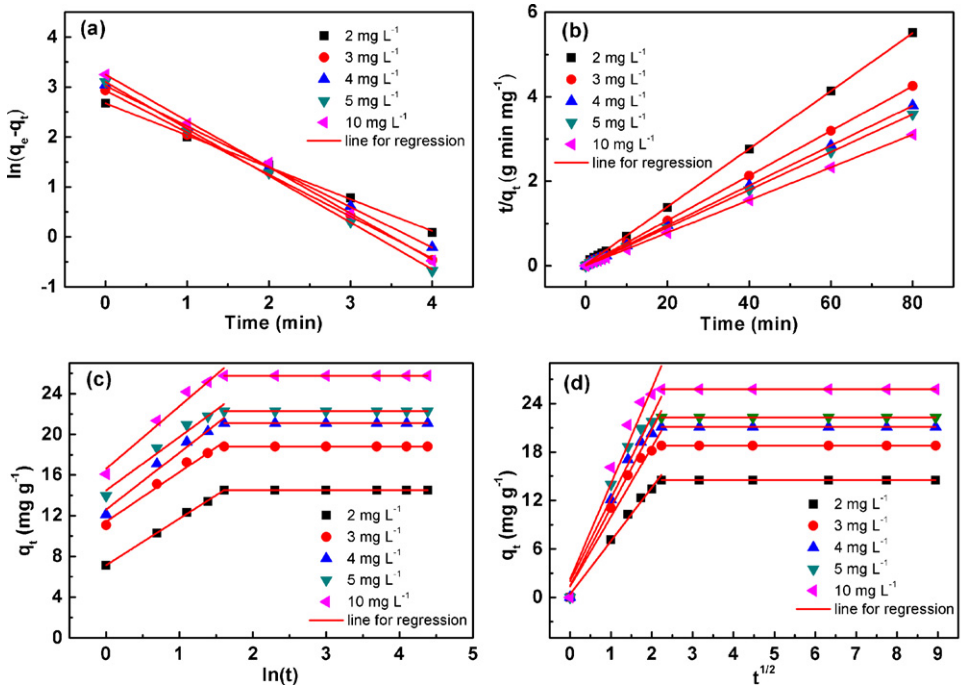

Fig. 2. The fitting of different kinetic models for Cu^{2+} adsorption onto MNP-NH_2 nanoparticles at different initial concentration (2 mg L^{-1}, 3 mg L^{-1}, 4 mg L^{-1}, 5 mg L^{-1} and 10 mg L^{-1}) at 25 °C ((a) Lagergren pseudo-first order, (b) Pseudo-second order, (c) Elovich, (d) Intra-particle diffusion).

Table 2
Kinetic parameters of different models for Cu^{2+} ions adsorption onto MNP-NH_2 nanoparticles.

Kinetic models and parameters	Cu^{2+} c_0 (mg L^{-1}) 2.0	3.0	4.0	5.0	10.0
q_e(exp.) (mg L^{-1})	14.50	18.81	21.13	22.30	25.82
Pseudo-first-order equation					
q_e(calc.) (mg L^{-1})	14.51	18.85	20.65	22.27	25.73
k_1 (min^{-1})	0.639	0.730	0.810	0.938	1.053
R^2	0.9984	0.9985	0.9997	0.9991	0.9992
SSE	0.197	0.205	0.116	0.135	0.188
Pseudo-second-order equation					
q_e(calc.) (mg L^{-1})	14.60	18.90	21.19	22.37	25.85
k_2 (g mg^{-1} min^{-1})	0.174	0.178	0.201	0.248	0.255
h (mg g^{-1} min^{-1})	37.97	62.30	90.09	124.07	170.08
R^2	0.9998	0.9998	0.9999	0.9999	0.9999
SSE	0.022	0.014	0.010	0.008	0.006
Elovich equation					
q_e(calc.) (mg L^{-1})	14.51	19.06	21.62	22.99	26.53
α (mg g^{-1} min^{-2})	21.77	35.39	53.02	81.88	139.09
β (g mg^{-1} min^{-1})	0.218	0.182	0.178	0.169	0.153
R^2	0.9988	0.9945	0.9711	0.9579	0.9417
SSE	0.078	0.194	0.474	0.542	0.666
Intra-particle diffusion equation					
q_e(calc.) (mg L^{-1})	14.77	19.26	21.66	22.87	26.26
k_{intra} (mg g^{-1} $min^{-1/2}$)	6.604	8.614	9.689	10.228	11.744
C	0.379	0.871	1.438	1.991	2.723
R^2	0.9898	0.9765	0.9525	0.9297	0.9078
SSE	0.442	0.882	1.425	1.848	2.453

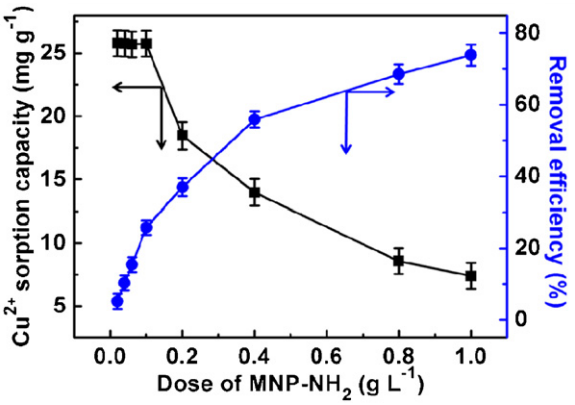

Fig. 3. Effect of amount of MNP-NH_2 on the removal of Cu^{2+} ions. Initial concentration of Cu^{2+} ion: 10 mg L^{-1}; pH 6.0; solution volume: 50 mL; temperature: 298 K. The bars represent the standard error of the mean.

and ln (t) were illustrated in Fig. 2(c). Before reaching the adsorption equilibrium, the plots exhibit relative good linear relationship. From their slopes and intercepts, Elovich constants were determined and given in Table 2.

The possibility of intra-particle diffusion was explored by using the intra-particle diffusion model represented by the Eq. (5). Where k_{intra} is the intra-particle diffusion rate constant (mg g^{-1} $min^{-1/2}$) and C is a constant related with the thickness of boundary layer (mg g^{-1}). If the plot of q_t *vs.* $t^{1/2}$ gives a straight line, the sorption process is controlled by intra-particle diffusion only. However, if the data exhibit multi-linear plots, then two or more steps influence the sorption process. Here the plot of q_t *vs.* $t^{1/2}$ for Cu^{2+} is shown in two stages (Fig. 2(d)). The first straight portion depicts macropore diffusion and the second representing micropore diffusion [38]. The calculated kinetic parameters k_{intra} and C were listed in Table 2. Significantly, the intercept (C) as proposed by Eq. (5) was not zero, indicating that intra-particle diffusion may not be the controlling factor in determining the kinetics of the process [38].

Although the values of calculated equilibrium capacities (q_e(calc.)) from the Lagergren pseudo-first order, pseudo-second order, Elovich and the intra-particle diffusion kinetic models were in agreement with those of experimental capacities (q_e(exp.)) at different initial Cu^{2+} concentrations to some extent (Table 2), it is probable that the adsorption system is not followed by the lagergren first-order or Elovich or intra-particle kinetic models. The higher correlation coefficients (R^2) and lower SSE values for pseudo-second-order kinetic model indicated that the sorption followed a pseudo-second order mechanism, and the sorption process was controlled by chemisorption [39].

3.2. Influence of amount of MNP-NH_2

An optimum adsorbent dose is essentially required to maximize the interactions between metal ions and adsorption sites of adsorbent in the solution [32]. To evaluate the optimum dosage of MNP-NH_2 adsorbent, 1.0–50.0 mg of freshly prepared MNP-NH_2 was added to 50.0 mL of aqueous solution containing 10.0 mg L^{-1} Cu^{2+}. Analysis of Fig. 3 demonstrated that the removal efficiencies of Cu^{2+} increased from 5% to 74% with increasing adsorbent amount, while the amount of Cu^{2+} adsorbed per unit mass, q_e, decreased from 25.80 to 7.39 mg g^{-1}. Increasing the dose of MNP-NH_2 would increase the number of available adsorption sites, thereby resulting in the increase in removal percentage of Cu^{2+}. The decrease in sorbent capacity may be due to interference between binding sites and higher adsorbed dose or insufficiency of metal ions in solution with respect to available binding sites [40]. Of course, it may be also due to aggregation resulting from high sorbent dose. Such aggregation would lead to a decrease in total surface area of the sorbent and an increase in diffusional path length [41]. The particle interaction at higher adsorbent concentration may also help to desorb some of the loosely bound metal ions from the sorbent surface [42]. Fig. 3 indicates that a sorbent concentration of 0.1 g L^{-1} would insure the best removal percentage and the best sorbent capacity.

3.3. Effect of initial pH on adsorption and zeta potential analyses

Acidity is one of the most important factors in the adsorption of environmental contaminants in aqueous solution since it can affect the solution chemistry of contaminants (i.e. hydrolysis, redox reactions, polymerization and coordination). Acidity also has a strong influence on the ionic state of functional groups on the surface of adsorbents [43]. Under different pH conditions, the removal efficiency of Cu^{2+} ions by the sorbent was detected. As presented in Fig. 4(a), the removal efficiency increased from 53% to 100% when the initial pH varied from 2 to 6, then kept at 100% with increasing pH. The variation of Cu^{2+} adsorption with solution pH could be explained by the following Eqs. (6) and (7), which described reactions took place at the solid-solution interface of MNP-NH_2 sorbent:

$$MNP - NH_2 + H^+ = MNP - NH_3^+ \quad (6)$$

$$MNP - NH_2 + Cu^{2+} = MNP - NH_2Cu^{2+} \quad (7)$$

Eq. (6) indicated the protonation and deprotonation reactions of MNP-NH_2 in solution, and Eq. (7) shown that Cu^{2+} ions formed complexes with the amino groups on the surface of MNP-NH_2. According to the Eq. (6), the reaction favored the protonation of NH_2 to form NH_3^+ at lower pH. As more NH_2 groups were protonated to form NH_3^+ cations, there were only fewer NH_2 binding sites on the surface of MNP-NH_2 for Cu^{2+} ions adsorption through Eq. (7). Furthermore, the electrostatic repulsion between Cu^{2+} ion and MNP-NH_2 increased with more NH_3^+ formed on the surface of MNP-NH_2. These effects decreased the adsorption of Cu^{2+} ions on the MNP-NH_2 with decreasing pH. Conversely, the reaction in Eq. (7) proceeded to the left with increasing solution pH, leading to an increase of the number of NH_2 sites on the surface of MNP-NH_2 for Cu^{2+} ion adsorption through Eq. (7) and thus increasing the sorption capacity [27,29]. It was supported that the isoelectric point (pI) of MNP-NH_2 was 5.8, revealing that amino-functionalized nanoparticles were positively charged at pH < 5.8 (Fig. 4(b)).

By comparison with MNP-NH_2, naked Fe_3O_4 nanoparticles (MNP) could only absorb significantly less Cu^{2+} ions under the same pH conditions. According to Fig. 4(b), the isoelectric point (pI) of naked nanoparticles was 5.4, which was close to that reported in literature [26] and similar with that of MNP-NH_2. However, there was a remarkable difference in removal efficiency of Cu^{2+} ions between MNP and MNP-NH_2, and MNP-NH_2 exhibited larger adsorption capacity than MNP. Considering the difference between MNP and MNP-NH_2, the larger adsorption capacity of MNP-NH_2 attributed to the amino groups modified on the surface of MNP-NH_2.

Considering the hydrolysis and precipitation of Cu^{2+}, the species formed in the pH range 3–6 are Cu^{2+} (unhydrolyzed species), $Cu(OH)^+$, and $Cu(OH)_2$ [44]. Among them Cu^{2+} is the predominant species in the solution, and the concentration of $Cu(OH)_2$ is very low and negligible. In addition, according to solubility product constant of $Cu(OH)_2$ ($\log(K_{sp}) = 19.66$) [45], $Cu(OH)_2$ precipitate forms when the concentration of Cu^{2+} is larger than 12 mg L^{-1} at pH 6.0. In this study, the largest concentration of Cu^{2+} is 10 mg L^{-1}, and no precipitation was observed. Therefore, the experiments in this study were performed at pH 6.0.

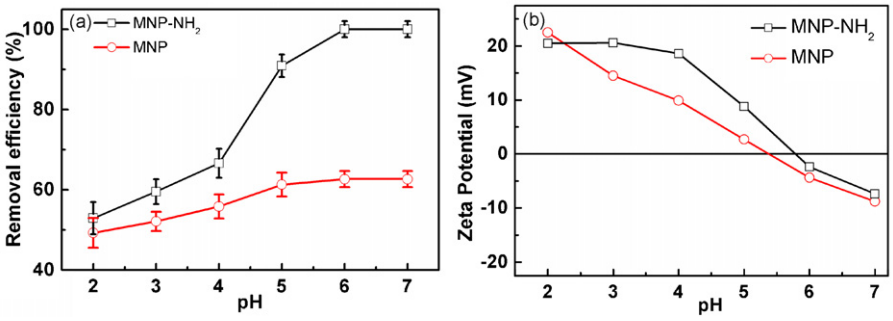

Fig. 4. (a) Effect of pH on Cu^{2+} adsorption on MNP-NH_2. Initial concentration of Cu^{2+}: 10 mg L^{-1}; MNP-NH_2: 5 mg; solution volume: 50 mL. (b). Zeta potentials of MNP and MNP-NH_2 at various pH values.

3.4. Adsorption isotherms

To understand the adsorption mechanism of Cu^{2+} ions on the nano-adsorbent, the adsorption data were analyzed by adsorption isothermal models. Here Langmuir, Freundlich and Dubinin–Radushkevich (D–R) adsorption isotherm models were used to describe the equilibrium between adsorbed Cu^{2+} on MNP-NH_2 (q_e) and Cu^{2+} in solution (C_e) at a constant temperature.

The Langmuir model assumes that adsorption takes place at specific homogeneous sites within the adsorbent and has found successful application in many monolayer adsorption processes. The linear form of the Langmuir isotherm is depicted by the following equation:

$$\frac{C_e}{q_e} = \frac{1}{K_L q_m} + \frac{C_e}{q_m} \quad (8)$$

where q_e represents the amount of Cu^{2+} adsorbed on the absorbent at equilibrium (mg g^{-1}); C_e describes the equilibrium Cu^{2+} concentration (mg L^{-1}); q_m denotes the maximum adsorption capacity corresponding to complete monolayer coverage and K_L is the Langmuir adsorption equilibrium constant (L mg^{-1}). Thus, a plot of C_e/q_e *vs.* C_e (Fig. 5) results in a straight line of slope ($1/q_m$) and an intercept of $1/K_L q_m$. From the slopes and intercepts, the values of q_m and K_L were calculated to be 25.77 mg g^{-1} and 2.41 L mg^{-1} respectively. The Table 3 present the comparison of adsorption capacity (mg g^{-1}) of MNP-NH_2 from the Langmuir isotherm for Cu^{2+} with that of various adsorbents reported in literature [8–14,16,17,21–23,26,27,31,32].

The type of the Langmuir isotherm can be used to predict whether the adsorption is favorable or unfavorable in term of either the equilibrium parameter or a dimensionless constant separation factor R_L, which is defined by the following equation [46]:

$$R_L = \frac{1}{1 + K_L C_0} \quad (9)$$

Here C_0 (mg L^{-1}) is the initial concentration of Cu^{2+}. The R_L indicates the type of isotherm to be irreversible ($R_L = 0$), favorable ($0 < R_L < 1$), linear ($R_L = 1$) or unfavorable ($R_L > 1$). The R_L values in this study were in the range from 4.17×10^{-2} to 0.806 (Table 3), which indicated the favorable adsorption between Cu^{2+} and MNP-NH_2 sorbent.

The Freundlich model is applied to monolayer adsorption as Langmuir model but not a saturation-type isotherm. It is used to estimate the sorption intensity of the adsorbent towards the adsorbate and it can be represented as follows:

$$\ln q_e = \ln K_F + \frac{1}{n} \ln C_e \quad (10)$$

where K_F is Freundlich constant indicating adsorption capacity, n is an empirical parameter related to the intensity of adsorption. The value of n varies with the heterogeneity of the adsorbent and for favorable adsorption process the value of n should lie in the range of 1–10 [47]. They can be calculated from the intercept and slope of linear plot of $\ln q_e$ *vs.* $\ln C_e$, respectively (figure not shown), and the values of K_F and n at different temperatures were shown in Table 4.

Moreover, the sorption data were applied to the D–R model in order to distinguish between physical and chemical adsorption. The linear form of the D–R model is:

$$\ln q_e = \ln q_{max} - \beta \varepsilon^2 \quad (11)$$

where β is the activity coefficient related to mean adsorption energy (mol^2 J^{-2}); q_e and C_e represent the same mean as above mentioned. q_{max} is the maximum adsorption capacity of Cu^{2+} ions on MNP-NH_2 corresponding to D–R monolayer coverage (mg g^{-1}); ε is the Polanyi potential (kJ^2 mol^{-2}), which can be obtained from the following relation:

$$\varepsilon = RT \ln\left(1 + \frac{1}{C_e}\right) \quad (12)$$

R is the gas constant (8.314 J mol^{-1} K^{-1}) and T is the temperature (K).

The experimental data were evaluated by plotting $\ln q_e$ against ε^2 to obtain the value of q_{max} and β from the intercept and slope, respectively. The mean sorption energy E (kJ mol^{-1}) is the free energy of the transfer per mole of the sorbate from infinity to the adsorbent surface and can be calculated using the following equation.

$$E = \frac{1}{\sqrt{2\beta}} \quad (13)$$

The magnitude of this parameter is useful for information about the type of adsorption process such as chemical ion exchange or

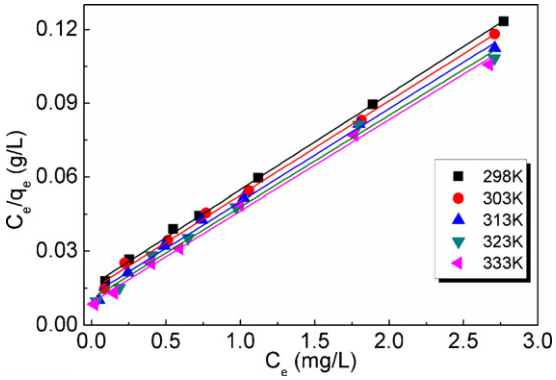

Fig. 5. Langmuir plots for the adsorption of Cu^{2+} onto MNP-NH_2 at different temperatures.

Table 3
Comparison of adsorption capacity of various adsorbents for Cu^{2+}.

Sorbents	Capacity ($mg\,g^{-1}$)	Refs.
Activated carbon modified by poly(N,N-dimethylaminoethyl methacrylate)	31.46	[8]
Carbon nanotubes	24.49	[9]
Crosslinked chitosan with epichlorohydrin	35.46	[10]
Oxidized coir	6.99	[11]
Unmodified coir	2.54	[11]
Silica gel microspheres encapsulated with 5-sulfosalicylic acid functionalized polystyrene	29.73	[12]
Sepiolite	38.17	[13]
Polyacrylonitrile/pumice composite	4.12	[14]
Microorganisms immobilized on composite polyurethane foam	28.74	[16]
Poly(hydroxyethyl methacrylate) nanobeads containing imidazole groups	58	[17]
Hydroxyapatite nanoparticles	36.9	[21]
Maghemite nanoparticle	27.7	[22]
Magnetic gamma-Fe_2O_3 nanoparticles coated with poly-L-cysteine	42.9	[23]
Fe_3O_4 magnetic nanoparticles coated with humic acid	46.3	[26]
Amino-functionalized magnetic nano-adsorbent	12.43	[27]
Magnetic nano-adsorbent modified by gum arabic	38.5	[29]
Chitosan-bound Fe_3O_4 magnetic nanoparticles	21.5	[31]
Magnetic nanoparticles coated by chitosan carrying of α-ketoglutaric acid	96.15	[32]
Amino-functionalized magnetic nanosorbent	25.77	This work

Table 4
Isotherm constants for the adsorption of Cu^{2+} onto MNP-NH_2 at various temperatures.

T (K)	Langmuir				Freundlich			Dubinin–Radushkevich (D–R)			
	q_m ($mg\,g^{-1}$)	K_L ($L\,mg^{-1}$)	R_L range	r^2_L	n	K_F ($L\,g^{-1}$)	r^2_F	q_{max} ($mg\,g^{-1}$)	β ($mol^2\,kJ^{-2}$)	r^2_{D-R}	E ($kJ\,mol^{-1}$)
298	25.77	2.41	0.0768–0.806	0.9972	2.31	16.69	0.9498	165.78	3.03×10^{-3}	0.9691	12.84
303	26.13	2.64	0.0703–0.791	0.9973	2.40	17.42	0.9567	155.78	2.80×10^{-3}	0.9717	13.34
313	26.48	3.20	0.0588–0.757	0.9954	2.59	18.39	0.9602	144.88	2.46×10^{-3}	0.9793	14.22
323	26.56	3.79	0.0502–0.725	0.9933	2.69	19.41	0.9407	133.87	2.17×10^{-3}	0.9645	15.18
333	26.58	4.60	0.0417–0.685	0.9961	2.81	20.25	0.9482	129.97	1.97×10^{-3}	0.9735	15.94

physical adsorption. When it lies between 8 and 16 $kJ\,mol^{-1}$, the adsorption occurs chemically, otherwise, the reaction proceeds physically as it smaller than 8 $kJ\,mol^{-1}$ [48]. All values of q_{max}, β and E were given in Table 4. It can be seen that the E values varied from 12.84 to 15.94 $kJ\,mol^{-1}$ at all studied temperatures, indicating that the adsorption of Cu^{2+} by MNP-NH_2 may be interpreted as chemical ion exchange adsorption. The E value at room temperature was consistent with some previous results [49–51].

The Langmuir, Freundlich and D–R parameters for the adsorption of Cu^{2+} onto nano-adsorbent were summarized in Table 4. It was evident that the Langmuir model fitted the experimental data better than the Freundlich and D–R models based on the r^2 values in Table 4.

3.5. Thermodynamic parameters

In any adsorption procedure, both energy and entropy considerations should be considered in order to determine what process will take place spontaneously. Values of thermodynamic parameters have the great significance for practical application of a process. The change in free energy ΔG^o, enthalpy ΔH^o and entropy ΔS^o associated with the adsorption process were calculated by using the following equations:

$$\Delta G^o = -RT\ln K \quad (14)$$

$$\ln K = -\frac{\Delta G^o}{RT} = -\frac{\Delta H^o}{RT} + \frac{\Delta S^o}{R} \quad (15)$$

where R is the gas constant (8.314 $J(mol\,K)^{-1}$), T the absolute temperature (K), K (q_e/C_e) an equilibrium constant at various temperatures [52]. ΔH^o and ΔS^o were calculated from the slope and intercept of the plot of $\ln K$ *vs.* $1/T$ (Fig. 6), and the values of ΔG^o, ΔH^o and ΔS^o were collected in Table 5. The negative values of ΔG^o confirmed that the adsorption was spontaneous, and the decreasing of ΔG^o as temperature rises indicated that the adsorption was more favorable at high temperatures. The positive value of ΔH^o confirmed the endothermic nature of adsorption which was also supported by the increase in value of Cu^{2+} uptake with the rise in temperature. The positive value of ΔS^o suggested the increasing randomness at the solid/liquid interface during the adsorption of Cu^{2+} ions on MNP-NH_2.

3.6. Influence of salinity

Increasing NaCl salinity from 0% to 3.5% (the salinity of seawater) had no effects on the removal of Cu^{2+} by MNP-NH_2. It suggested that no interaction occurred among NaCl, MNP-NH_2 and Cu^{2+}, and the complexation of Cu^{2+} with Cl^- was much weaker than the coordination between Cu^{2+} and amino groups on the surface of MNP-NH_2.

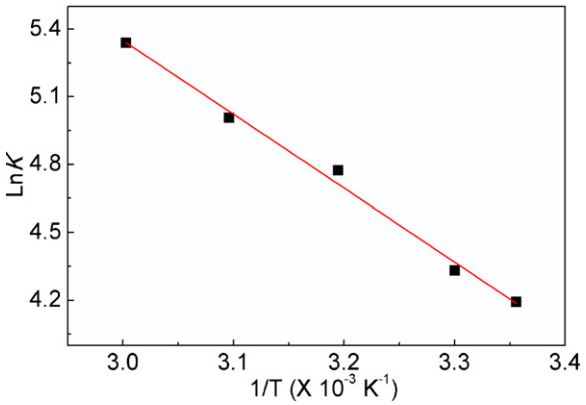

Fig. 6. Plot of $\ln K$ *vs.* $1/T$ to predict thermodynamic parameters for the adsorption of Cu^{2+} ions onto MNP-NH_2.

Table 5
Thermodynamic parameters of Cu^{2+} adsorption onto MNP-NH_2 at different temperatures.

T (K)	$\ln K$ (L mg^{-1})	ΔG^o (kJ mol^{-1})	ΔH^o (kJ mol^{-1})	ΔS^o (J (mol K)$^{-1}$)
298	4.19	−10.39	27.18	126.1
303	4.33	−10.91		
313	4.77	−12.42		
323	5.01	−13.44		
333	5.34	−14.78		

Table 6
The pH, concentration of COD, and Cu^{2+} in water and the removal (%) after treating 50 mL of water with 0.1 g L^{-1} MNP-NH_2 sorbent. (Remove efficiency ± S.D.).

Matrix	pH	COD (mg L^{-1})	$Cu^{2+}{}_{initial}$ (mg L^{-1})	$Cu^{2+}{}_{removal}$ (%)
Tap water	6.5	3	1.001 ± 0.042	98 ± 0.090
Polluted river	6.1	30	1.005 ± 0.060	98 ± 0.010

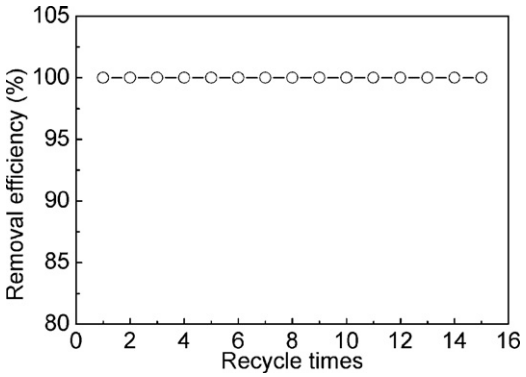

Fig. 7. Regeneration studies of MNP-NH_2.

3.7. Real water matrix and coexisted ions

The river polluted by industrial wastewater and tap water spiked with 1.0 mg L^{-1} Cu^{2+} were used to evaluate practical application of MNP-NH_2. Table 6 shows the initial concentration and the removal efficiencies of Cu^{2+} after treatment with MNP-NH_2. For the studied water samples, the observed removals of Cu^{2+} were 98% and were hardly influenced by the commonly coexisted ions in industrial wastewater or in tap water. It is evident that coexisted ions in natural water, such as Ca^{2+} and Mg^{2+}, have no influence on the removal efficiency of Cu^{2+} with MNP-NH_2. Furthermore, our experiments indicated that Pb^{2+} and Ni^{2+} have little effect on Cu^{2+} adsorption (data not shown), and further work is needed to explore the influence of other heavy metal ions.

3.8. Reusability of MNP-NH_2 for Cu^{2+} removal

Taking into account the practical application, the adsorption–desorption cycle was repeated 15 times using the same nanoparticles. Analysis of the influence of pH on the removal efficiency, it was expected that acid would be an effective agent for desorption.

The results indicated that Cu^{2+} ions could be desorbed completely by 1 min sonication in the presence of 0.1 mol L^{-1} HCl. In addition, the performance and reproducibility of regenerated MNP-NH_2 retained unchanged in the following adsorption. Fig. 7 showed the relationship between the time for reuse and the adsorption efficiency of the regenerated nanoabsorbent. It can be seen that the adsorption capacity of MNP-NH_2 kept constantly and no difference in desorption capacity was observed during 15 sorption–desorption cycles. These results are encouraging and suggest that nano-adsorbent in this study has good reusability. Since 0.1 mol L^{-1} HCl solution was used as the desorbing agent and the nano-adsorbent was dried in an oven during regeneration, each adsorption–desorption process must go with an acid-treated process and a heat-treated process. Thus, the reproducibility of MNP-NH_2 displayed in Fig. 7 also indicated its good stability. The excellent reusability and stability indicate that MNP-NH_2 has a great potential in practical application.

4. Conclusions

In this study, MNP-NH_2 has been prepared facilely by one-pot method and been characterized by transmission electron microscopy, X-ray diffraction, FT-IR spectrum, laser particle size analysis and zeta potential. Adsorption studies of Cu^{2+} ions onto MNP-NH_2 led to the following conclusions.

(1) Various factors affecting the uptake behavior such as contact time, temperature, pH, salinity, amount of MNP-NH_2 and initial concentration of Cu^{2+} were evaluated. The adsorption process was relatively fast and the equilibrium could be reached within 5 min, and the maximum adsorption of Cu^{2+} ions occurred at pH 6 and 298 K. Increasing NaCl from 0% to 3.5% (the salinity of seawater) had no effects on the adsorption of Cu^{2+} on MNP-NH_2.
(2) Kinetic models including the Lagergren first-order, pseudo-second-order, Elovich and intra-particle diffusion were applied to the experimental data. The adsorption was found to follow the pseudo-second-order model, and chemical sorption was the rate-limiting step.
(3) The equilibrium data were still analyzed using the Langmuir, Freundlich, and Dubinin–Radushkevich isotherm models. It was found that the sorption of Cu^{2+} ions was well fitted to the Langmuir equation with maximum monolayer adsorption capacity of 25.77–26.58 mg g^{-1} at 298–333 K. The values of the adsorption energy, E (kJ mol^{-1}), varied from 12.84 to 15.94 kJ mol^{-1} at all studied temperatures (298–333 K), indicating that the adsorption of Cu^{2+} by MNP-NH_2 may be interpreted as chemical adsorption. Thermodynamic parameters revealed that the adsorption was spontaneous and endothermic in nature.
(4) Most importantly, MNP-NH_2 exhibited a high stability and good reusability under experimental conditions. Copper ions could be desorbed completely by 0.1 mol L^{-1} HCl solution within 1 min, and the regenerated MNP-NH_2 could retain the original metal removal level. MNP-NH_2 was able to remove 98% of Cu^{2+} from industrial wastewater and tap water. The 15 adsorption–desorption cycles suggested that the nano-adsorbent in this study had a great potential in practical application.

Acknowledgements

This work was supported by the National Basic Research Program of China (973 Program) 2006CB705601, the President Fund of GUCAS. Thanks for the financial support from the State Key Laboratory of Environmental Chemistry and Ecotoxicology, Research Center for Eco-Environmental Sciences, Chinese Academy of Sciences.

Appendix A. Supplementary data

Supplementary data associated with this article can be found, in the online version, at doi:10.1016/j.jhazmat.2010.08.048.

References

[1] J.S. Espana, E.L. Pamo, E.S. Pastor, J.R. Andres, J.A.M. Rubi, The removal of dissolved metals by hydroxysulphate precipitates during oxidation and neutralization of acid mine waters, Aquat. Geochem. 12 (2006) 269–298.

[2] M.G. da Fonseca, M.M. de Oliveora, L.N.H. Arakaki, J.G.P. Espinola, C. Airoldi, Natural vermiculite as an exchanger support for heavy cations in aqueous solution, J. Colloid Interface Sci. 285 (2005) 50–55.
[3] O. Arous, A. Gherrou, H. Kerdjoudj, Removal of Ag(I), Cu(II) and Zn(II) ions with a supported liquid membrane containing cryptands as carriers, Desalination 161 (2004) 295–303.
[4] U.B. Ogutveren, S. Koparal, E. Ozel, Electrodialysis for the removal of copper ions from wastewater, J. Environ. Sci. Health A 32 (1997) 749–761.
[5] S.H. Hasan, P. Srivastava, Batch and continuous biosorption of Cu^{2+} by immobilized biomass of Arthrobacter sp, J. Environ. Manage. 90 (2009) 3313–3321.
[6] Y. Sag, Y. Aktay, Kinetic studies on sorption of Cr(VI) and Cu(II) ions by chitin, chitosan and Rhizopus arrhizus, Biochem. Eng. J. 12 (2002) 143–153.
[7] J.C. Zheng, H.M. Feng, M.H.W. Lam, P.K.S. Lam, Y.W. Ding, H.Q. Yu, Removal of Cu(II) in aqueous media by biosorption using water hyacinth roots as a biosorbent material, J. Hazard. Mater. 171 (2009) 780–785.
[8] S.M. Zhu, N. Yang, D. Zhang, Poly(N,N-dimethylaminoethyl methacrylate) modification of activated carbon for copper ions removal, Mater. Chem. Phys. 113 (2009) 784–789.
[9] G.P. Rao, C. Lu, F. Su, Sorption of divalent metal ions from aqueous solution by carbon nanotubes: a review, Sep. Purif. Technol. 58 (2007) 224–231.
[10] A.H. Chen, S.C. Liu, C.Y. Chen, C.Y. Chen, Comparative adsorption of Cu(II), Zn(II), and Pb(II) ions in aqueous solution on the crosslinked chitosan with epichlorohydrin, J. Hazard. Mater. 154 (2008) 184–191.
[11] S.R. Shukla, V.G. Gaikar, R.S. Pai, U.S. Suryavanshi, Batch and column adsorption of Cu(II) on unmodified and oxidized coir, Sep. Sci. Technol. 44 (2009) 40–62.
[12] P. Yin, Q. Xu, R.J. Qu, G.F. Zhao, Removal of transition metal ions from aqueous solutions by adsorption onto a novel silica gel matrix composite adsorbent, J. Hazard. Mater. 169 (2009) 228–232.
[13] M. Dogan, A. Turkyilmaz, M. Alkan, O. Demirbas, Adsorption of copper (II) ions onto sepiolite and electrokinetic properties, Desalination 238 (2009) 257–270.
[14] M. Yavuz, F. Gode, E. Pehlivan, S. Ozmert, Y.C. Sharma, An economic removal of Cu^{2+} and Cr^{3+} on the new adsorbents: pumice and polyacrylonitrile/pumice composite, Chem. Eng. J. 137 (2008) 453–461.
[15] R. Rangsivek, M.R. Jekel, Removal of dissolved metals by zero-valent iron (ZVI): kinetics, equilibria, processes and implications for stormwater runoff treatment, Water Res. 39 (2005) 4153–4163.
[16] L.C. Zhou, Y.F. Li, X. Bai, G.H. Zhao, Use of microorganisms immobilized on composite polyurethane foam to remove Cu(II) from aqueous solution, J. Hazard. Mater. 167 (2009) 1106–1113.
[17] D. Turkmen, E. Yilmaz, N. Ozturk, S. Akgol, A. Denizli, Poly(hydroxyethyl methacrylate) nanobeads containing imidazole groups for removal of Cu(II) ions, Mater. Sci. Eng. C 29 (2009) 2072–2078.
[18] S. Pacheco, R. Rodriguez, Adsorption properties of metal ions using alumina nano-particles in aqueous and alcoholic solutions, J. Sol-Gel Sci. Technol. 20 (2001) 263–273.
[19] F.M. Koehler, M. Rossier, M. Waelle, E.K. Athanassiou, L.K. Limbach, R.N. Grass, D. Günther, W.J. Stark, Magnetic EDTA: coupling heavy metal chelators to metal nanomagnets for rapid removal of cadmium, lead and copper from contaminated water, Chem. Commun. (Cambridge) (2009) 4862–4864.
[20] Y.H. Li, J. Ding, Z.K. Luan, Z.C. Di, Y.F. Zhu, C.L. Xu, D.H. Wu, B.Q. Wei, Competitive adsorption of Pb^{2+}, Cu^{2+} and Cd^{2+} ions from aqueous solutions by multiwalled carbon nanotubes, Carbon 41 (2003) 2787–2792.
[21] Y.J. Wang, J.H. Chen, Y.X. Cui, S.Q. Wang, D.M. Zhou, Effects of low-molecular-weight organic acids on Cu(II) adsorption onto hydroxyapatite nanoparticles, J. Hazard. Mater. 162 (2009) 1135–1140.
[22] J. Hu, G.H. Chen, I.M.C. Lo, Selective removal of heavy metals from industrial wastewater using maghemite nanoparticle: Performance and mechanisms, J. Environ. Eng.—ASCE 132 (2006) 709–715.
[23] B.R. White, B.T. Stackhouse, J.A. Holcombe, Magnetic gamma-Fe_2O_3 nanoparticles coated with poly-L-cysteine for chelation of As(III), Cu(II), Cd(II), Ni(II), Pb(II) and Zn(II), J. Hazard. Mater. 161 (2009) 848–853.
[24] Y.F. Shen, J. Tang, Z.H. Nie, Y.D. Wang, Y. Ren, L. Zuo, Preparation and application of magnetic Fe_3O_4 nanoparticles for wastewater purification, Sep. Sci. Technol. 68 (2009) 312–319.
[25] Y.F. Shen, J. Tang, Z.H. Nie, Y.D. Wang, Y. Ren, L. Zuo, Tailoring size and structural distortion of Fe_3O_4 nanoparticles for the purification of contaminated water, Bioresour. Technol. 100 (2009) 4139–4146.
[26] J.F. Liu, Z.S. Zhao, G.B. Jiang, Coating Fe_3O_4 magnetic nanoparticles with humic acid for high efficient removal of heavy metals in water, Environ. Sci. Technol. 42 (2008) 6949–6954.
[27] S.H. Huang, D.H. Chen, Rapid removal of heavy metal cations and anions from aqueous solutions by an amino-functionalized magnetic nano-adsorbent, J. Hazard. Mater. 163 (2009) 174–179.
[28] W. Yantasee, C.L. Warner, T. Sangvanich, R.S. Addleman, T.G. Carter, R.J. Wiacek, G.E. Fryxell, C. Timchalk, M.G. Warner, Removal of heavy metals from aqueous systems with thiol functionalized superparamagnetic nanoparticles, Environ. Sci. Technol. 41 (2007) 5114–5119.
[29] S.S. Banerjee, D.H. Chen, Fast removal of copper ions by gum arabic modified magnetic nano-adsorbent, J. Hazard. Mater. 147 (2007) 792–799.
[30] J.Y. Tseng, C.Y. Chang, C.F. Chang, Y.H. Chen, C.C. Chang, D.R. Ji, C.Y. Chiu, P.C. Chiang, Kinetics and equilibrium of desorption removal of copper from magnetic polymer adsorbent, J. Hazard. Mater. 171 (2009) 370–377.
[31] Y.C. Chang, D.H. Chen, Preparation and adsorption properties of monodisperse chitosan-bound Fe_3O_4 magnetic nanoparticles for removal of Cu(II) ions, J. Colloid Interface Sci. 283 (2005) 446–451.
[32] Y.T. Zhou, H.L. Nie, C. Branford-White, Z.Y. He, L.M. Zhu, Removal of Cu^{2+} from aqueous solution by chitosan-coated magnetic nanoparticles modified with alpha-ketoglutaric acid, J. Colloid. Interface Sci. 330 (2009) 29–37.
[33] L.Y. Wang, J. Bao, L. Wang, F. Zhang, Y.D. Li, One-pot synthesis and bioapplication of amine-functionalized magnetite nanoparticles and hollow nanospheres, Chem. Eur. J. 12 (2006) 6341–6347.
[34] S. Lagergren, About the theory of so called adsorption of soluble substances, Ksver Veterskapsakad Handl. 24 (1898) 1–6.
[35] Y.S. Ho, G. McKay, Pseudo-second order model for sorption processes, Process Biochem. 34 (1999) 451–465.
[36] S.H. Chien, W.R. Clayton, Application of Elovich equation to the kinetics of phosphate release and sorption in soils, Soil Sci. Soc. Am. J. 44 (1980) 265–268.
[37] Y.S. Ho, G. McKay, Sorption of dye from aqueous solution by peat, Chem. Eng. J. 70 (1998) 115–124.
[38] R.R. Sheha, A.A. El-Zahhar, Synthesis of some ferromagnetic composite resins and their metal removal characteristics in aqueous solutions, J. Hazard. Mater. 150 (2008) 795–803.
[39] C. Araneda, C. Fonseca, J. Sapag, C. Basualto, M. Yazdani-Pedram, K. Kondo, E. Kamio, F. Valenzuela, Removal of metal ions from aqueous solutions by sorption onto microcapsules prepared by copolymerization of ethylene glycol dimethacrylate with styrene, Sep. Purif. Technol. 63 (2008) 517–523.
[40] T. Fan, Y. Liu, B. Feng, G. Zeng, C. Yang, M. Zhou, H. Zhou, Z. Tan, X. Wang, Biosorption of cadmium (II), zinc (II) and lead (II) by *Penicillium simplicissimum*: isotherms, kinetics and thermodynamics, J. Hazard. Mater. 160 (2008) 655–661.
[41] Z. Rawajfih, N. Nsour, Thermodynamic analysis of sorption isotherms of chromium (VI) anionic species on reed biomass, J. Chem. Thermodyn. 40 (2008) 846–851.
[42] S. Erenturk, E. Malkoc, Removal of lead(II) by adsorption onto *Viscum album* L.: effect of temperature and equilibrium isotherm analyses, Appl. Surf. Sci. 253 (2007) 4727–4733.
[43] Y.M. Ren, X.Z. Wei, M.L. Zhang, Adsorption character for removal Cu(II) by magnetic Cu(II) ion imprinted composite adsorbent, J. Hazard. Mater. 158 (2008) 14–22.
[44] F.M. Doyle, Z.D. Liu, The effect of triethylenetetraamine (Trien) on the ion flotation of Cu^{2+} and Ni^{2+}, J. Colloid. Interface Sci. 258 (2003) 396–403.
[45] J.G. Speight, Lange's Handbook of Chemistry, 16th ed., McGraw–Hill, New York, 2005.
[46] K.R. Hall, L.C. Eagleton, A. Acrivos, T. Vermeulen, Pore- and solid-diffusion kinetics in fixed-bed adsorption under constant-pattern conditions, Ind. Eng. Chem. Fundam. 5 (2) (1966) 212–223.
[47] T. Fan, Y.G. Liu, B.Y. Feng, G.M. Zeng, C.P. Yang, M. Zhou, H.Z. Zhou, Z.F. Tan, X. Wang, Biosorption of cadmium(II), zinc(II) and lead(II) by *Penicillium simplicissimum*: Isotherms, kinetics and thermodynamics, J. Hazard. Mater. 160 (2008) 655–661.
[48] F. Helfferich, Ion Exchange, McGraw-Hill, New York, 1962.
[49] P. Miretzky, C. Munoz, A. Carrillo-Chavez, Cd (II) removal from aqueous solution by *Eleocharis acicularis* biomass, equilibrium and kinetic studies, Bioresour. Technol. 101 (2010) 2637–2642.
[50] M. Tuzen, A. Sari, Biosorption of selenium from aqueous solution by green algae (*Cladophora hutchinsiae*) biomass: Equilibrium, thermodynamic and kinetic studies, Chem. Eng. J. 158 (2010) 200–206.
[51] M. Wawrzkiewicz, Z. Hubicki, Weak base anion exchanger amberlite fpa51 as effective adsorbent for acid blue 74 removal from aqueous medium - kinetic and equilibrium studies, Sep. Sci. Technol. 45 (2010) 1076–1083.
[52] Z.Y. Yao, J.H. Qi, L.H. Wang, Equilibrium, kinetic and thermodynamic studies on the biosorption of Cu (II) onto chestnut shell, J. Hazard. Mater. 174 (2010) 137–143.